DOI: 10.21062/mft.2021.075  http://www.journalmt.com

# Effect of Boronizing Process of AISI 321 Stainless Steel Surface on its Corrosion Resistance in Acid Environments (pH = 1)

Karina Jagielska-Wiaderek (0000-0002-6230-8532)
Czestochowa University of Technology, Faculty of Production Engineering and Materials Technology. Armii Krajowej 19, Częstochowa 42-217, Poland. E-mail: jagielska-wiaderek.karina@wip.pcz.pl

**The paper presents results of research under the effect of surface thermo-chemical treatment on the corrosion resistance of X6CrNiTi18-10 steel. The corrosion resistance of the surface layers of stainless steel obtained as a result of thermo-chemical treatment (boronizing process) was assessed using the method of progressive thinning, which consists in performing corrosion tests on deeper and deeper areas of the surface layer. This method allowed for the determination of changes in individual characteristic corrosion parameters read from the potentiokinetic polarization curves and the determination of the depth profiles of these parameters. In the paper, results of tests of X6CrNiTi18-10 steel resistance to general corrosion, performed in acidified sulphate solutions (pH = 1) have been presented. The thickness of the surface layer was assessed on the basis of structural tests and changes in microhardness on the cross-section of the material. It has been found that the extremely high hardness of the boron layer was accompanied by deterioration of the corrosion resistance. The general corrosion rate of the surface layer is 3-4 times higher than the corrosion rate of the material core (substrate). The characteristics of the passive state of steel are particularly worsened, which is manifested by an increase in the value of the critical passivation current, the minimum current in the passive range and by limiting the tendency to secondary passivation.**

**Keywords:** corrosion, stainless steel, boride layers, AISI, boronizing process

## 1 Introduction

All engineering constructions are subject to design optimization in terms of their intended use and the selection of materials for their manufacturing. The essential optimization criteria are, first of all, production costs, quality requirements, functional properties and environmental impacts (manufacturing and end-of-life phase) [1–3]. The functional properties include: properties resulting from the structure and chemical composition of materials, (i.e. mechanical, corrosion resistance), as well as properties resulting from the processing of the entire material or surface treatment (i.e., tibological properties and variability of properties with respect to treatment parameters) [4].

Due to the wide range of applications as well as the wide range of possibilities of shaping the mechanical, tribological and other properties of austenitic stainless steels, their use is constantly growing [5]. The growing interest in this type of steels is also determined by the possibility of subjecting stainless steels to various methods of thermal, chemical or chemical-thermal treatment [6–8]. One of the methods of increasing the durability of structural elements that is applicable to austenitic steels is saturation of the surface with boron. The result of this process is the production of surface layers with high hardness and abrasion resistance [9–12]. Typical layers of boron saturated steel are characterized by the presence of FeB boride in the near-surface zone. The hardness of such a layer can reach values close to 2300 HV. In the deeper layers, in the structure are present $Fe_2B$ borides with a slightly lower hardness, the hardness of such a layer can reach values close to 1800 HV [9, 13]. Due to the content of chromium and nickel in the chemical composition of austenitic steels, after the borinizing process, CrB, $Cr_2B$, NiB and $Ni_2B$ may also be present in the surface layer. Chromium and nickel borides also have a significant impact on improving the properties of the surface layer [14]. The properties of the boron-saturated layer are of course determined by the parameters of the boronizing process (temperature, time, concentration of the treatment atmosphere). As the temperature and time of the chemical-thermal process increase, the thickness of the boron layer increases (i.e. borides appear at a greater depth) – the boride layer growth kinetics is characterized by a parabolic curve [15]. Consequently, it causes a significant increase in hardness and wear resistance, but unfortunately reduces the resistance to plastic deformation and contributes to the propagation of surface cracks [15–17].

Due to the interaction of materials with the utility environment, corrosion tests have for years been the

basis for assessing the usefulness of engineering materials in terms of their durability and reliability - this applies to numerous groups of materials widely described in the literature [10, 18–23], For austenitic stainless steels, it is also one of the criteria for the effectiveness of property optimization. Most of the tests of this type of steel concern very aggressive corrosive media, especially strongly acidic and containing high concentrations of chloride ions [21, 22].

The aim of this study is to characterize the structure, mechanical properties and the corrosion resistance of the layer obtained as a result of X6CrNiTi18-10 steel boronizing. Corrosion resistance in strongly acidic environment. However, these characteristics will not refer (as usual) to the properties on the surface of the detail, but to the depth of the surface layer. For this purpose, the method of progressive thinning has been used in the study, and the measurements were performed at various depths of the surface layer. This method makes it possible to obtain a profile for the performance parameters of the boron saturated layer.

## 2 Experimental procedure

The subject of the research were samples of austenitic steel type X6CrNiTi18-10, the surface of which was saturated with boron. The boronizing process was carried out at 900 °C for 6 hours, using the gas-contact method in the mixture of KBF4, aluminium oxide and "Ekabor" powders - as a source of boron.

Metallographic tests were carried out on the cross-section of the surface layer using optical (Neophot 32) and scanning (Jeol 6610 LV) microscopes. The chemical composition analysis was performed for selected layer depths using the EDS analyzer. The hardness distribution in the surface layer was measured using the Vickers method, with a load of 0.4903N (HV0.05).

Potentiokinetic polarization curves were performed in 0.5M sulphate solutions acidified to pH = 1. During the measurements, the solutions were deaerated with argon. Samples for electrochemical tests have the form of rotating discs with a working area of 0.2 $cm^2$. Before each potentiodynamic measurement, parallel layers 4÷10 μm thick were grounded from the surface of the disc electrodes, shifting to the core of the material. The average thickness of the grounded layer was determined on the basis of the weight loss of the tested electrode in relation to the initial mass with an accuracy of ± 0.02 mg. The methodology adopted in analogy to the other works [24–26] - method of progressive thinning.

Potentiokinetic studies were performed at the temperature of 25 ± 0.1 °C, at the rotation speed equal to 12 rpm and at the scanning speed of the potential of 5 $mVs^{-1}$, using its shift from the corrosion potential ($E_{corr}$) to the value of $E_f$ = 1.7 V. Before the polarization tests, the samples were immersed in a corrosive solution for 0.5 hours in order to establish the stationary potential (Open Circuit Potential (OCP)). All electrode potentials are relative to the 1M silver chloride electrode.

## 3 Results and discussion

In Fig. 1 exemplary images of the microstructure obtained on the cross-section of the boride layers on the X6CrNiTi18-10 steel have been presented. It is known [9, 27–30] that the thickness and phase composition of boron layers are strictly dependent on the applied parameters of the thermo-chemical treatment. As can be seen from Fig. 1, during the boronizing process (at 900 °C for 6 hours), a typical three-zone surface layer was obtained, where under the MB-type boron particles layer distinguish the $M_2B$-type partitions layer, which then passes into the diffusion zone.

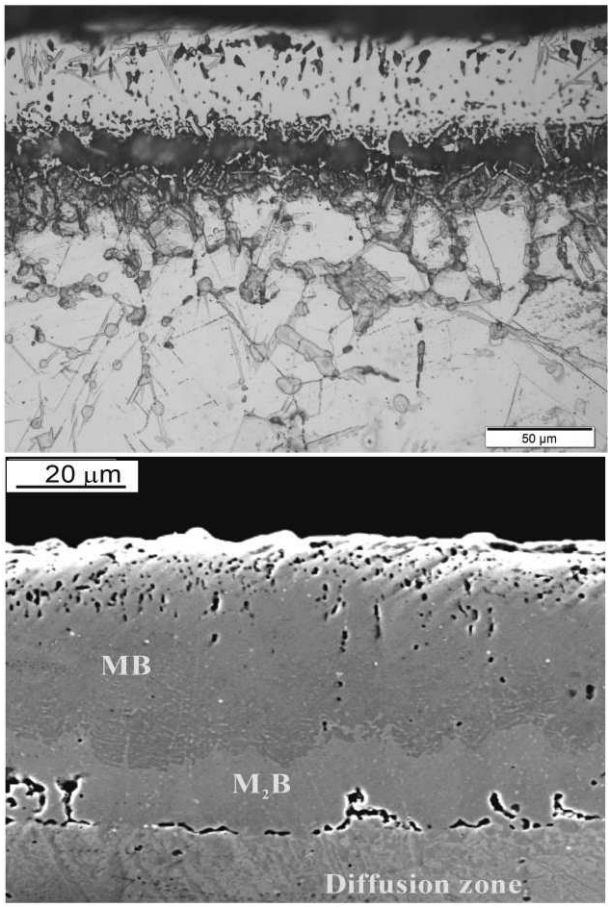


***Fig. 1*** *Microstructure on the cross-section of the surface layer of X6CrNiTi18-10 steel after boronizing process (900 °C, 6 h, in the mixture of KBF4)*

The performed point analyses of the chemical composition for different depths of the layer (Fig. 2) showed the boron content in the outer zone is about 16-19% by weight, while for the deeper areas it is ap-

prox. 9-11% by weight. This confirms the zonal presence of FeB and $Fe_2B$ precipitates, for which the stoichiometric boron content is 16.23% for FeB and 8.83% for $Fe_2B$ [31]. It should also be noted that due to the increased content of chromium and nickel in the tested steel, apart from the typical iron borides (FeB and $Fe_2B$), the structure may also include precipitations: CrB, $Ni_2B$ and $(Fe,M)_2B$, where M = Cr or Ni) [8, 32–34]. With the applied process parameters (at 900 °C for 6 hours), structural changes are observed up to a depth of approx. 70-80 μm. It was also observed that boride layers are characterized by the sawtooth-like morphology, which is characteristic of these layers and widely described by Delai et al. and Rodríguez-Castro et al. [15, 35].

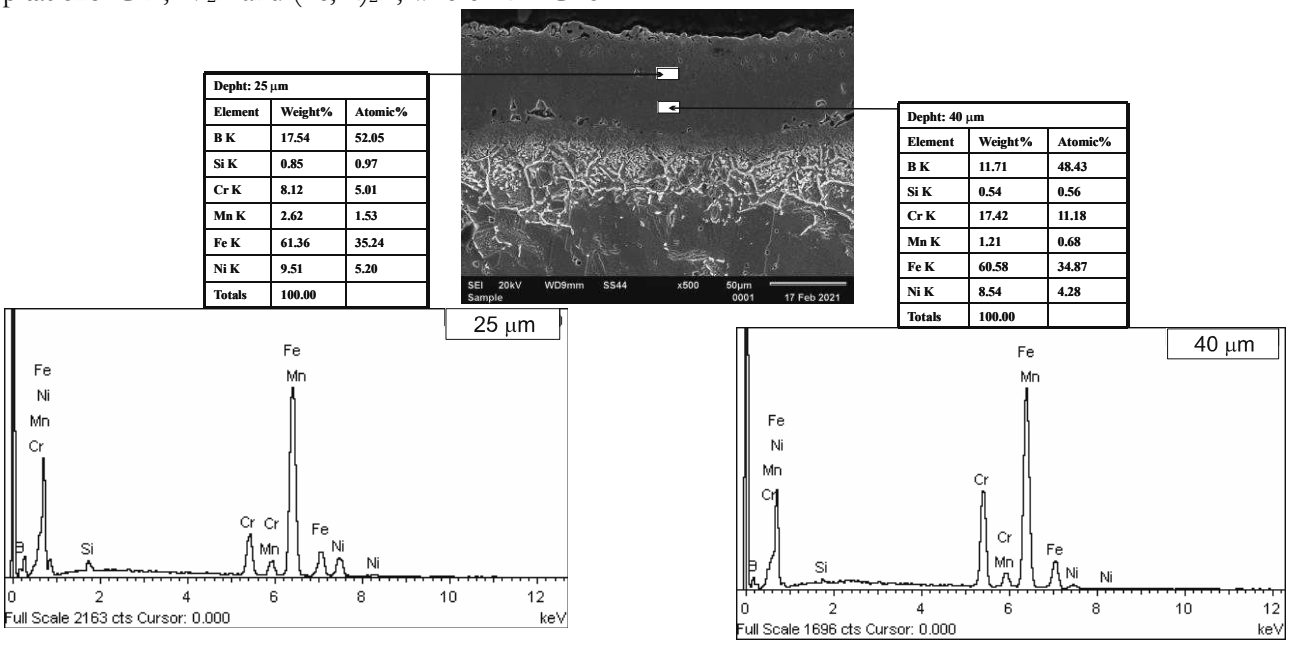


***Fig. 2*** *EDS spectra shown on the cross-section of the sample treated at 900° for 6 h associated with the results of X-ray microanalysis: FeB layer (25 μm) and $Fe_2B$ layer (40 μm)*

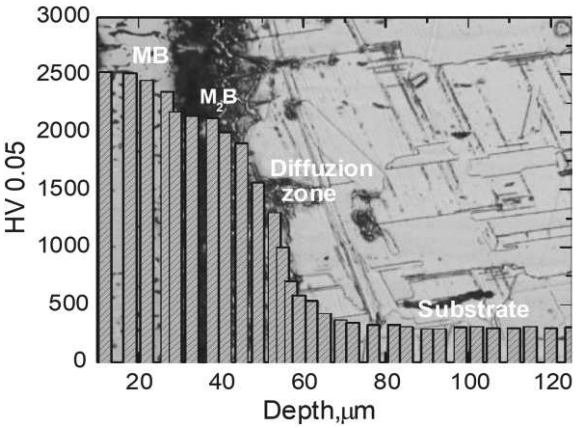


***Fig. 3*** *Microhardness of boronized AISI 321 steel as a function of distance from the surface*

In order to be able to observe changes in hardness between individual zones of the boride layer, hardness measurements were made on the cross-section of the surface layer. As shown in Fig. 3, hardness increase occurs up to a depth of approx. 70 ÷ 80 μm, i.e. to the depth to which changes in the material structure were observed (Fig. 1). The greatest hardening, by over 2000 HV 0.05 units, occurs down to a depth of approx. 35 μm, and the hardness obtained in this area proves the presence of FeB and CrB borides [11]. The second zone of the boride layer (depth from 35 to 55 μm) includes $M_2B$ borides, therefore the obtained hardness values assume lower values (1400 ÷ 2000 HV0.05), which is characteristic for this type of precipitates [31]. At depths> 50 μm, i.e. in the diffusion zone, the hardness of the material clearly decreases, finally assuming the value of approx. 300 HV0.05 for a depth of 75 μm - characteristic for the material core (X6CrNiTi18-10 steel) [25, 30, 36, 37]

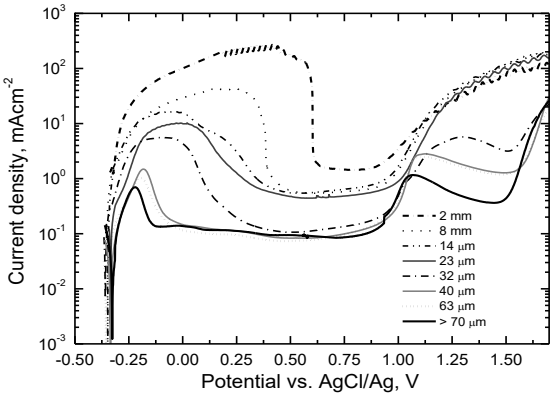


***Fig. 3*** *Potentiodynamic polarization curves for the boronized AISI 321 steel and grounded to a specific depth (μm), obtained from a 0.5 M sulphate solution (pH = 1). Experimental conditions: 25± 0,1°C, electrode stirring 12 rps, potential scan rate 5 mVs-1).*

The anodic polarization curves of boronized stainless steel determinated in pH = 1 are shown in Fig. 4. The obtained series of curves characterize the corrosive behaviour of the material at several depths from the surface. For the clarity of the chart, out of several dozen of polarization curves made for successive depths, only curves for a few selected depths have been shown.

As shown in Fig. 3, saturation of the X6CrNiTi18-10 steel surface with boron does not affect the value of the corrosion potential, regardless of the analysed layer depth, this value remains constant at $E_{corr}$ = -0.3V. For potentials values higher than $E_{corr}$, the curves in the anode range are closely dependent on the analysed depth. For steel without treatment, after exceeding the potential $E$ = –0.2 V, a clear decrease in the anode current is observed, which should be related to the effective passivation of the steel surface. However, the boronized surface of the X6CrNiTi18-10 steel behaves differently: above -0.2V it does not passivate but it develops intensively up to the potential of +0.5V, only in the range from +0.5 to + 0.9V it shows a small section, not too effective passive state. A clear influence of surface saturation with boron is also visible at higher values of the potentials, while in the transpassive range the tested material has a tendency to secondary passivation, and the borne surface spreads in the transpassive range at a high speed.

The next potentiokinetic curves recorded for deeper and deeper layers of the material are characterized in particular by a systematic decrease in the critical passivation current ($i_{cp}$) as well as the minimum anode current in the passive range ($i_{min.p}$). Fig. 4 shows the depth profiles of both these parameters. A strong decrease in $i_{cp}$ as well as a slightly smaller $i_{min.p}$ in the applied corrosive solution is observed up to a depth of about 35-40 μm, i.e. at depths where MB-type separations dominate in the structure (see Fig. 1).

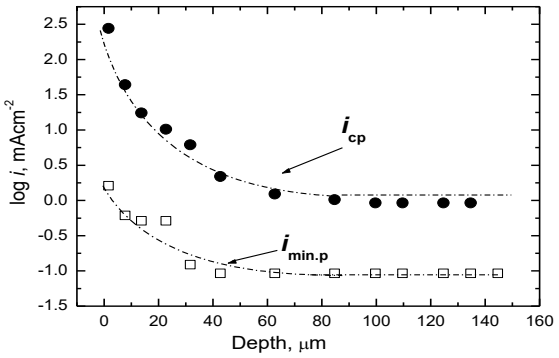


***Fig. 4*** *Depth profiles of the critical passivation current ($i_{cp}$) and the minimum current within the passive range ($i_{min.p}$)*

A detailed analysis of the polarization curves presented in Fig. 3 allows to find differences in the dissolution rates of the material at different depths of the surface layer. In this study, the extrapolation method was used to determine the $i_{corr}$ (0.12 V was selected as the slope of the tangents) and the extrapolation was carried out to the cathode-anode transition potential, which was assumed as the corrosion potential.

For the shallowest zones of the borne layer, where MB-type separations are dominant, $i_{corr}$ has the highest values, about 3 m·Acm$^{-2}$. With the increase in the depth of the layer and the change in its structure, the corrosion rate systematically decreases, and for the M2B precipitation zone, the corrosion current values are m·Acm$^{-2}$., and for the diffusion zone and the material core, 0.1 m·Acm$^{-2}$.

## 4 Conclusion

- Saturation of the X6CrNiTi18-10 steel surface with boron leads to the formation of a strongly hardened surface layer reaching a depth of approx. 70-80 μm. The obtained layer shows a zonal structure, and the strongest hardening is observed up to a depth of approx. 35 μm, where MB-type separations dominate in the structure.
- Corrosion resistance is closely related to the zonal structure of the boron layer. The application of the progressive thinning method allows to track changes in corrosion resistance over the entire cross-section of the surface layers. The enrichment of the steel surface with boron the strongest deteriorates its corrosion resistance in the outermost areas of the layer.
- The characteristics of the passive and transpassive states deteriorate significantly: the saturation of the layer with hydrogen causes an increase in the value of the critical passivation current and a slightly smaller increase in the minimum current density in the passive range.

## References

[1] STANISZEWSKA, E., KLIMECKA-TATAR, D., OBRECHT, M. (2020). Eco-design processes in the automotive industry. In: *Production Engineering Archives*, Vol. 26, No. 4, pp. 131–137, doi: 10.30657/pea.2020.26.25.

[2] ABIDI, Y. (2021). Analysis of the compromise between cutting tool life, productivity and roughness during turning of C45 hardened steel. In: *Production Engineering Archives*, Vol. 27, No. 1, pp. 30–35, doi: 10.30657/pea.2021.27.4.

[3] ZHANG, Q., HU, J., FENG, J., LIU, A. (2020). A novel multiple criteria decision making method for material selection based on GGPFWA operator. In: *Materials & Design*,

Vol. 195, No. 8, 109038, doi: 10.1016/j.matdes.2020.109038.

[4] TEPLICKÁ, K., HURNÁ, S. (2021). New Approach of Costs of Quality According their Trend of During Long Period in Industrial Enterprises in SMEs. In: *Management Systems in Production Engineering*, Vol. 29, No. 1, pp. 20–26, doi: 10.2478/mspe-2021-0003.

[5] JIA, S., TAN, Q., YE, J., ZHU, Z., JIANG, Z. (2021). Experiments on dynamic mechanical properties of austenitic stainless steel S30408 and S31608. In: *Journal of Constructional Steel Research*, Vol. 179, No. 2, 106556, doi: 10.1016/j.jcsr.2021.106556.

[6] VICEN, M., BOKŮVKA, O., NIKOLIĆ, R., BRONČEK, J. (2020). Tribological behavior of low-alloyed steel after nitriding. In: *Production Engineering Archives*, Vol. 26, No. 3, pp. 78–83, doi: 10.30657/pea.2020.26.16.

[7] KUSMIČ, D., ČECH, O., KLAKURKOVÁ, L. (2021). Corrosion Resistance of Ferritic Stainless Steel X12Cr13 After Application of Low-Temperature and High-Temperature Plasma Nitriding. In: *Manufacturing Technology*, Vol. 21, No. 1, pp. 98–104, doi: 10.21062/mft.2021.013.

[8] LIPIŃSKI, T., ULEWICZ, R. (2021). The effect of the impurities spaces on the quality of structural steel working at variable loads. In: *Open Engineering*, Vol. 11, No. 1, pp. 233–238, doi: 10.1515/eng-2021-0024.

[9] KUL, M., DANACI, I., GEZER, Ş., KARACA, B. (2020). Effect of boronizing composition on hardness of boronized AISI 1045 steel. In: *Materials Letters*, Vol. 279, 128510, doi: 10.1016/j.matlet.2020.128510.

[10] PANDA, J.N., WONG, B.C., MEDVEDOVSKI, E., EGBERTS, P. (2021). Enhancement of tribo-corrosion performance of carbon steel through boronizing and BN-based coatings. In: *Tribology International*, Vol. 153, pp. 1–12, 106666, doi: 10.1016/j.triboint.2020.106666.

[11] KEDDAM, M., CHEGROUNE, R., KULKA, M., MAKUCH, N., PANFIL, D., SIWAK, P., TAKTAK, S. (2018). Characterization, Tribological and Mechanical Properties of Plasma Paste Borided AISI 316 Steel. In: *Transactions of the Indian Institute of Metals*, Vol. 71, No. 1, pp. 79–90, doi: 10.1007/s12666-017-1142-6.

[12] IVANOV, O., PRYSYAZHNYUK, P., LUTSAK, D., MATVIIENKIV, O., AULIN, V. (2020). Improvement of Abrasion Resistance of Production Equipment Wear Parts by Hardfacing with Flux-Cored Wires Containing Boron Carbide/Metal Powder Reaction Mixtures. In: *Management Systems in Production Engineering*, Vol. 28, No. 3, pp. 178–183, doi: 10.2478/mspe-2020-0026.

[13] GÜNEN, A., KURT, B., SOMUNKIRAN, İ., KANCA, E., ORHAN, N. (2015). The effect of process conditions in heat-assisted boronizing treatment on the tensile and bending strength characteristics of the AISI-304 austenitic stainless steel. In: *The Physics of Metals and Metallography*, Vol. 116, No. 9, pp. 896–907, doi: 10.1134/S0031918X15090021.

[14] KULKA, M., MAKUCH, N., DZIARSKI, P., PIASECKI, A. (2014). A study of nanoindentation for mechanical characterization of chromium and nickel borides' mixtures formed by laser boriding. In: *Ceramics International*, Vol. 40, No. 4, pp. 6083–6094, doi: 10.1016/j.ceramint.2013.11.059.

[15] DELAI, O., XIA, C., SHIQIANG, L. (2021). Growth kinetics of the FeB/Fe2B boride layer on the surface of 4Cr5MoSiV1 steel: experiments and modelling. In: *Journal of Materials Research and Technology*, Vol. 11, No. 7, pp. 1272–1280, doi: 10.1016/j.jmrt.2021.01.109.

[16] ARTEAGA-HERNANDEZ, L.A., CUAO-MOREU, C.A., GONZALEZ-RIVERA, C.E., ALVAREZ-VERA, M., ORTEGA-SAENZ, J.A., HERNANDEZ-RODRIGUEZ, M.A.L. (2021). Study of boriding surface treatment in the tribological behavior of an AISI 316L stainless steel. In: *Wear*, Vol. 69, 203825, doi: 10.1016/j.wear.2021.203825.

[17] CAMPOS, I., PALOMAR, M., AMADOR, A., GANEM, R., MARTINEZ, J. (2006). Evaluation of the corrosion resistance of iron boride coatings obtained by paste boriding process. In: *Surface and Coatings Technology*, Vol. 201, No. 6, pp. 2438–2442, doi: 10.1016/j.surfcoat.2006.04.017.

[18] HAYAJNEH, M.T., ALMOMANI, M., AL-DARAGHMEH, M. (2019). Enhancement the Corrosion Resistance of AISI 304 Stainless Steel by Nanocomposite Gelatin-Titanium Dioxide Coatings. In: *Manufacturing Technology*, Vol. 19, No. 5, pp. 759–766, doi: 10.21062/ujep/368.2019/a/1213-2489/MT/19/5/759.

[19] KLIMECKA-TATAR, D., PAWŁOWSKA, G., RADOMSKA, K. (2014). The effect of Nd12Fe77Co5B6 powder electroless biencapsulation method on atmospheric corrosion of polymer bonded magnetic material, *METAL 2014 - 23rd International Conference on Metallurgy and Materials*, 23rd International Conference on Metallurgy and Materials, METAL 2014 (23 May 2104, Brno, Czech Repubic), pp. 985–990.

[20] KLIMECKA-TATAR, D., RADOMSKA, K., PAWLOWSKA, G. (2015). Corrosion resistance, roughness and structure of Co64Cr28Mo5(Fe, Si, Al, Be)3 and Co63Cr29Mo6.5(C, Si, Fe, Mn)1.5 biomedical alloys. In: *Journal of the Balkan Tribological Association*, Vol. 21, No. 1, pp. 204–210.

[21] ZATKALÍKOVÁ, V., MARKOVIČOVÁ, L., BELAN, J., LIPTÁKOVÁ, T. (2014). Variability of Local Corrosion Attack Morphology of AISI 316Ti Stainless Steel in Aggressive Chloride Environment. In: *Manufacturing Technology*, Vol. 14, No. 3, pp. 493–497, doi: 10.21062/ujep/x.2014/a/1213-2489/MT/14/3/493.

[22] ZATKALÍKOVÁ, V., MARKOVIČOVÁ, L. (2019). Influence of temperature on corrosion resistance of austenitic stainless steel in cl − containing solutions. In: *Production Engineering Archives*, Vol. 25, No. 25, pp. 43–46, doi: 10.30657/pea.2019.25.08.

[23] LIPIŃSKI, T. (2021). Investigation of corrosion rate of X55CrMo14 stainless steel at 65% nitrate acid at 348 K. In: *Production Engineering Archives*, Vol. 27, No. 2, pp. 108–111, doi: 10.30657/pea.2021.27.13.

[24] JAGIELSKA-WIADEREK, K., BALA, H., WIECZOREK, P., RUDNICKI, J., KLIMECKA-TATAR, D. (2009). Corrosion resistance depth profiles of nitrided layers on austenitic stainless steel produced at elevated temperatures. In: *Archives of Metallurgy and Materials*, Vol. 54, No. 1, pp. 115–120.

[25] JAGIELSKA-WIADEREK, K. (2019). Depth Corrosion Characteristics of Borided Layer Produced on AISI 321 Stainless Steel. In: *Acta Physica Polonica A*, Vol. 135, No. 2, pp. 252–255, doi: 10.12693/APhysPolA.135.252.

[26] JAGIELSKA-WIADEREK, K., BALA, H., WIERZCHON, T. (2013). Corrosion depth profiles of nitrided titanium alloy in acidified sulphate solution. In: *Open Chemistry, Central European Journal of Chemistry*, Vol. 11, No. 12, pp. 2005–2011, doi: 10.2478/s11532-013-0342-0.

[27] ARAZ, S.O., GUMUS, H., BAYCA, S.U., AYDIN, A. (2021). Investigation of gamma-ray attenuation coefficients for solid boronized 304l stainless steel. In: *Applied radiation and isotopes including data, instrumentation and methods for use in agriculture, industry and medicine*, Vol. 170, 109605, doi: 10.1016/j.apradiso.2021.109605.

[28] ÇETIN, M., GÜNEN, A., KALKANDELEN, M., KARAKAŞ, M.S. (2021). Microstructural, wear and corrosion characteristics of boronized AISI 904L superaustenitic stainless steel. In: *Vacuum*, Vol. 187, No. 5, 110145, doi: 10.1016/j.vacuum.2021.110145.

[29] JAGIELSKA-WIADEREK, K. (2019). The structure and corrosion resistance of the cross-section of the boronized AISI 321 stainless steel. In: *Ochrona przed korozją*, Vol. 62, No. 11, pp. 372–375, doi: 10.15199/40.2019.11.2.

[30] KASANA, S.S., PANDEY, O.P. (2021). Effect of heat treatment on microstructure and mechanical properties of boron containing Ti-Stabilized AISI-321 steel for nuclear power plant application. In: *Materials Today Communications*, Vol. 26, No. 1948, 101959, doi: 10.1016/j.mtcomm.2020.101959.

[31] PRZYBYŁOWICZ, K. (2000). *Teoria i praktyka borowania stali*, Wydawnictwo Politechniki Świętokrzyskiej (in Polish), Kielce.

[32] LEE, S.Y., KIM, G.S., KIM, B.-S. (2004). Mechanical properties of duplex layer formed on AISI 403 stainless steel by chromizing and boronizing treatment. In: *Surface and Coatings Technology*, 177-178, pp. 178–184, doi: 10.1016/j.surfcoat.2003.07.009.

[33] ŞAHIN, S. (2009). Effects of boronizing process on the surface roughness and dimensions of AISI 1020, AISI 1040 and AISI 2714. In: *Journal of Materials Processing Technology*, Vol. 209, No. 4, pp. 1736–1741, doi: 10.1016/j.jmatprotec.2008.04.040.

[34] CALIK, A., SAHIN, O., UCAR, N. (2009). Mechanical Properties of Boronized AISI 316, AISI 1040, AISI 1045 and AISI 4140 Steels. In: *Acta Physica Polonica A*, Vol. 115, No. 3, pp. 694–698, doi: 10.12693/APhysPolA.115.694.

[35] RODRÍGUEZ-CASTRO, G., CAMPOS-SILVA, I., CHÁVEZ-GUTIÉRREZ, E., MARTÍNEZ-TRINIDAD, J., HERNÁNDEZ-SÁNCHEZ, E., TORRES-HERNÁNDEZ, A. (2013). Mechanical properties of FeB and Fe2B layers estimated by Berkovich nanoindentation on tool borided steel. In: *Surface and Coatings Technology*, Vol. 215, pp. 291–299, doi: 10.1016/j.surfcoat.2012.05.145.

[36] BRICÍN, D., KŘÍŽ, A. (2021). Influence of the Boriding Process on the Properties and the Structure of the Steel S265 and the Steel X6CrNiTi18-10. In: *Manufacturing Technology*, Vol. 21, No. 1, pp. 37–44, doi: 10.21062/mft.2021.003.

[37] BRNIC, J., TURKALJ, G., CANADIJA, M., LANC, D., KRSCANSKI, S., BRCIC, M., LI, Q., NIU, J. (2016). Mechanical properties, short time creep, and fatigue of an austenitic steel. In: *Materials*, Vol. 9, No. 4, doi: 10.3390/ma9040298.